

Note 3447

July 7, 1997

Routing of Clear Fibers

and

Architecture of the Front End Crates

By

Manuel I. Martin

Routing of Clear Fibers and Architecture of Front End Crates

Routing of Clear Fibers	1
and	1
Architecture of the Front End Crates	1
Introduction	3
1. Signals Path to the CFT Trigger Card.	3
2. Routing of Clear Fibers.	5
2.1 Naïve Layout.	5
2.1.1 Clear Fiber's Lengths Outside the Platform.	5
2.1.2 Clear Fiber's Length Inside the Platform.....	8
2.1.3 Total Clear Fiber's Lengths.	8
2.2 Five - Fold Symmetry Layout.....	10
2.2.1 Clear Fiber's Lengths between SF and MBs.	11
2.2.2 Clear Fiber's Lengths between the MBs and the VLPCs.	12
2.2.3 Total Clear Fiber's lengths.	13
3. Proposal for New Optical Fibers' Layout.....	13
3.1 Clear Fibers' Lengths between the SF and VLPCs.....	16
4. Time Arrival of Signals to Trigger Boards. Delays.....	17
4.1 Time Differences due to Particles' Trajectory: d_1 and d_2	17
4.1.1 Differences due to Particle Paths (d_1).	17
4.1.2 Differences due to Effective SF Length (d_2).....	18
4.1.3 Difference between Direct and Reflected Paths (Δd_2).....	19
4.1.4 Combination of both ($d_1 + d_2$).	20
4.2 Other Delays Independent of Clear Fibers' Routing.....	20
4.3 Time Differences due to Routing of Clear Fibers.....	21
4.4 Total Delays and Time Differences.....	21
5. Making Sense of the Numbers.....	22
5.1 Trigger Board Timing Requirements.	22
5.1.1 Data Acquisition by the Trigger Board.....	22
5.1.2 When to Start the Trigger Time.....	24
6. Comparison of Routing Schemes.	25
6.1 Comparison with the Naïve Layout.	25
6.2 Comparison between 5-fold and 4-fold geometry.	26

Introduction

Previous D0 Notes shown the way to transfer data, generated in the Scintillation Fibers, to the FPLDs where the CFT Trigger was generated. No specific mention of how the signals are routed from the CFT to the Trigger Boards was made. No timing information was given other than to show that the transfer from the PLDs to the FPLDs was made in four distinctive time slices. This note will attempt to address both of these issues. Accordingly, the note is divided into two major sections:

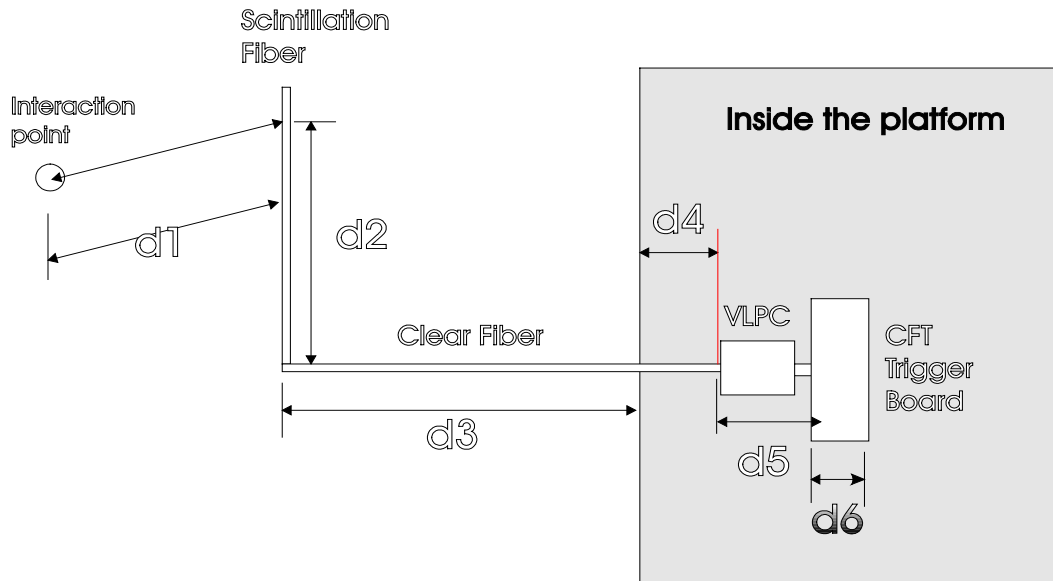
- 1) section 1 is dedicated to the study of the routing of signals from the SF to the crates where the VLPCs are located
- 2) section 2 will present the timings involved with the routing schemes unfolded on the previous section
- 3) section 3 will interpret the values obtained in the previous section, particularly as they relate to the Trigger Board timing scheme
- 4) section 4 will give some comparisons between the schemes shown and will end with some recommendations.

Before start it is convenient to give some general description of the elements and terminology used here.

1. Signals Path to the CFT Trigger Card.

Signals generated in the CFT as result of a proton anti-proton collision will arrive to the CFT Trigger Boards at different times because the paths traveled by them are different. To know the differences in path lengths is to know the differences in arrival times to the Trigger electronics. A simplified representation of the path taken by a 'signal' is shown on Fig. 1

Figure 1



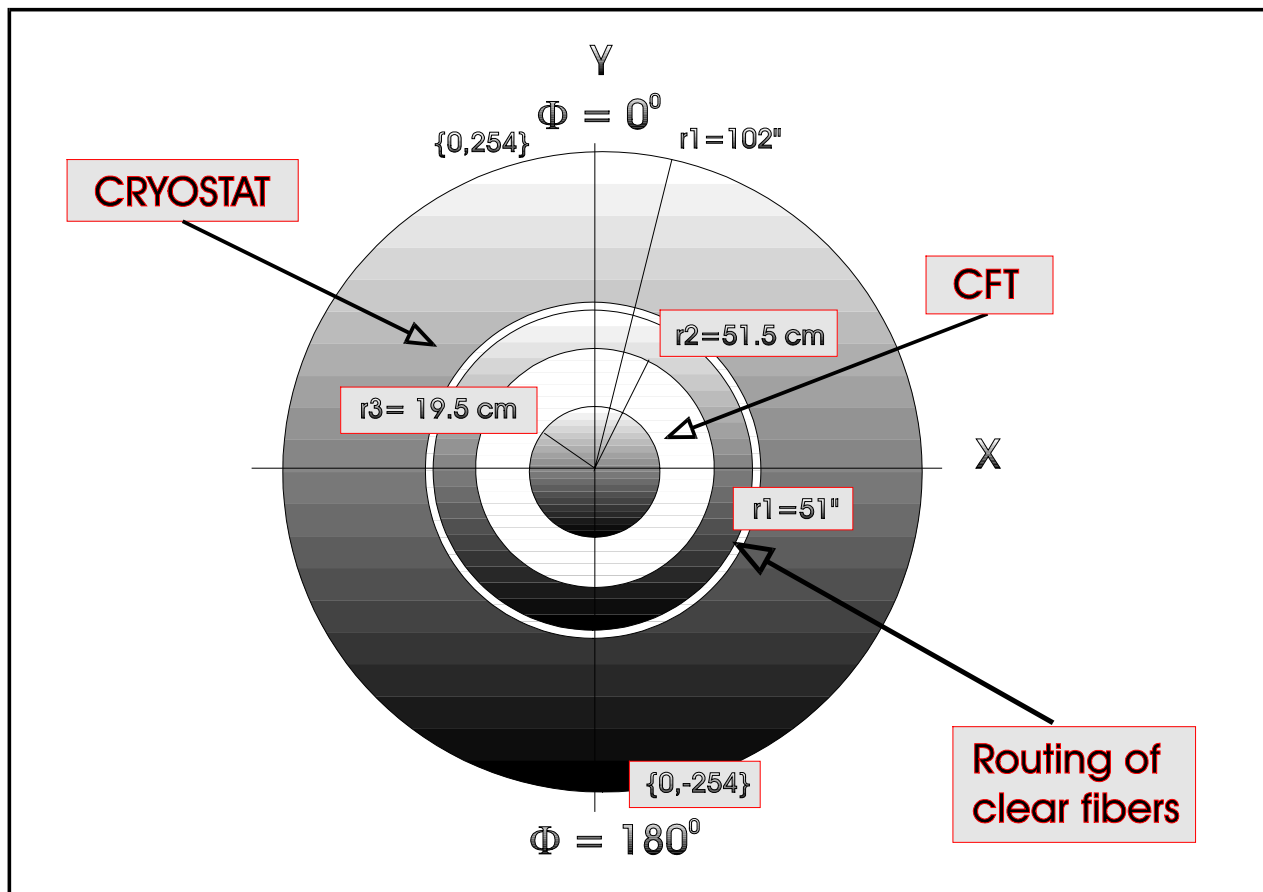
Routing of Clear Fibers and Architecture of Front End Crates

where $\{d1, d2, d3, d4, d5, d6\}$ correspond to the different path lengths travel by the signal (particle) from the point of origin to the input to the 'routing' PLD. These lengths will be given in cm or ns. The definitions of the different paths are as follows:

- 1) **d1** path followed by a particle originating at the interaction point until it strikes a scintillation fiber
- 2) **d2** path from the point where a particle strikes a scintillation fiber to the connection to the corresponding clear fiber. Two values of $d2$ must be considered: a direct path and a reflected path
- 3) **d3** length of the clear fiber up to the platform
- 4) **d4** length of the clear fiber inside the platform
- 5) **d5** delay in the VLPC and cable connecting the VLPC output to the CFT Trigger Board
- 6) **d6** delay incurred by the signals in the CFT Trigger Board from the input connector to the input of the corresponding 'routing' PLD.

For all practical purposes **d5** is the same for all signals with a value of ~ 2.3 ns.

Figure 2



The calculations will be made in two steps. First the length of the clear fibers will be obtained using three different rules for their physical layout. Second the total path length for the signals will be calculated.

2. Routing of Clear Fibers.

The three physical layouts to be used are:

- 1) a naïve layout where each clear fiber has a length dictated by the path followed by it and no bundles or other groupings of individual fibers are taken in account.
- 2) a layout following a five-fold symmetry is considered. Only a finite number of different possible clear fiber lengths are used
- 3) a layout proposed in this D0 Note where the sector organization of the CFT Trigger is conserved. A finite number of different possible clear fiber lengths is also used

2.1 Naïve Layout.

We will start by routing each clear fiber along a ‘logical’ path but without any consideration to mechanical interference between fibers or to possible bundling of them.

2.1.1 Clear Fiber’s Lengths Outside the Platform.

For the first rough calculations, the clear fibers are assumed to follow a path of constant Φ from the point of contact to the SF to half way to the outer surface of the Central Calorimeter Cryostat (see Fig. 2). At the surface of the Central Calorimeter Cryostat, the fibers continue along a circumference until they reach its lowest point at $\Phi=180^0$, $Z\sim 50$. From this point the fibers follow a radial path to the outer surface of the Central Calorimeter Cryostat and they drop to one hole on the floor located at $X \sim 30$, $Z \sim 50$. From this point on, they follow a sinuous path until they finally are connected to the VLPCs located on the platform of the detector at $Z \sim 0$ and from $X \sim 0$ to $X \sim 70$.

With these simplifications the signals path $\{d1, d2, d3, d4, d5, d6\}$ can be divided in two groups: a) fixed length paths and b) variable length paths. Furthermore, $\{d2\}$ can be divided in two distinctive sections:

- 1) a fixed portion $d3_{\text{fixed}}$ from $\Phi=180^0$, $Z\sim 50$ to the entrance to the platform where the VLPCs are located.
- 2) a variable portion $d3_{\text{variable}}$ from the boundary between SF and clear fiber to the point on the surface of the CCC with $\Phi=180^0$, $Z\sim 50$. The length of tis portion depends on the location of the SF.

The fixed portion $d3_{\text{fixed}}$ is given as follows

30*2.54 cm

along the X axis

Routing of Clear Fibers and Architecture of Front End Crates

$$\begin{array}{ll} (22 + 54.25 + 28.25)*2.54 \text{ cm} & \text{along the Y axis} \\ 50*2.54 \text{ cm} & \text{along the Z axis} \end{array}$$

$$\text{Total } d3_{\text{fixed}} = 184.5*2.54 = 468.63 \text{ cm.}$$

The variable portion of the length of the clear fibers is a function of the position of the corresponding SF in F as well as its layer assignment. These lengths are given by the expression

$$d3_{\text{variable}} = a_i + (R - r_i) + \pi \frac{|\phi_j - 180|}{180} R + R$$

where:

$i = \{A, B, C, D, E, F, G, H\}$ is the layer index, $j = \{1, \dots, 80\}$ is the sector index, a_i is the length of clear fiber needed to go from the boundary with the SF to the outer surface of the CCC, r_i is the radius of layer i and Φ_j is the Φ position of sector j and R is one half the radius of the CCC.

The values used are as follows:

$$\begin{array}{ll} a_A, a_B & = 47*2.54 = 119.38 \text{ cm} \\ a_{\{C,\dots,H\}} & = 4*2.54 = 10.16 \text{ cm} \\ R & = 51*2.54 = 129.54 \text{ cm} \end{array}$$

The following table shows $d3_{\text{variable}}$ for sectors from $\Phi = 0^0$ to $\Phi = 180^0$.

From it the following statistics are obtained:

$$\text{Maximum length} = 765.92 \text{ cm}$$

$$\text{Minimum length} = 227.91 \text{ cm}$$

$$\text{Average Length} = 459.49 \text{ cm}$$

Table 1

Layer	A	B	C	D	E	F	G	H	
Layer Radius	19.5	23.41	28.09	32.77	37.46	42.14	48.75	51.5	
Φ	Sector #	Clear fiber between the SF and a fixed point F = 180, Z = 50							
0.0	1	765.92	762.01	648.11	643.43	638.74	634.06	627.45	624.70
4.5	2	755.75	751.84	637.94	633.26	628.57	623.89	617.28	614.53
9.0	3	745.57	741.66	627.76	623.08	618.39	613.71	607.10	604.35
13.5	4	735.40	731.49	617.59	612.91	608.22	603.54	596.93	594.18
18.0	5	725.23	721.32	607.42	602.74	598.05	593.37	586.76	584.01
22.5	6	715.05	711.14	597.24	592.56	587.87	583.19	576.58	573.83
27.0	7	704.88	700.97	587.07	582.39	577.70	573.02	566.41	563.66
31.5	8	694.70	690.79	576.89	572.21	567.52	562.84	556.23	553.48
36.0	9	684.53	680.62	566.72	562.04	557.35	552.67	546.06	543.31
40.5	10	674.36	670.45	556.55	551.87	547.18	542.50	535.89	533.14
45.0	11	664.18	660.27	546.37	541.69	537.00	532.32	525.71	522.96
49.5	12	654.01	650.10	536.20	531.52	526.83	522.15	515.54	512.79
54.0	13	643.83	639.92	526.02	521.34	516.65	511.97	505.36	502.61
58.5	14	633.66	629.75	515.85	511.17	506.48	501.80	495.19	492.44
63.0	15	623.49	619.58	505.68	501.00	496.31	491.63	485.02	482.27
67.5	16	613.31	609.40	495.50	490.82	486.13	481.45	474.84	472.09
72.0	17	603.14	599.23	485.33	480.65	475.96	471.28	464.67	461.92
76.5	18	592.96	589.05	475.15	470.47	465.78	461.10	454.49	451.74
81.0	19	582.79	578.88	464.98	460.30	455.61	450.93	444.32	441.57
85.5	20	572.62	568.71	454.81	450.13	445.44	440.76	434.15	431.40
90.0	21	562.44	558.53	444.63	439.95	435.26	430.58	423.97	421.22
94.5	22	552.27	548.36	434.46	429.78	425.09	420.41	413.80	411.05
99.0	23	542.09	538.18	424.28	419.60	414.91	410.23	403.62	400.87
103.5	24	531.92	528.01	414.11	409.43	404.74	400.06	393.45	390.70
108.0	25	521.74	517.83	403.93	399.25	394.56	389.88	383.27	380.52
112.5	26	511.57	507.66	393.76	389.08	384.39	379.71	373.10	370.35
117.0	27	501.40	497.49	383.59	378.91	374.22	369.54	362.93	360.18
121.5	28	491.22	487.31	373.41	368.73	364.04	359.36	352.75	350.00
126.0	29	481.05	477.14	363.24	358.56	353.87	349.19	342.58	339.83
130.5	30	470.87	466.96	353.06	348.38	343.69	339.01	332.40	329.65
135.0	31	460.70	456.79	342.89	338.21	333.52	328.84	322.23	319.48
139.5	32	450.53	446.62	332.72	328.04	323.35	318.67	312.06	309.31
144.0	33	440.35	436.44	322.54	317.86	313.17	308.49	301.88	299.13
148.5	34	430.18	426.27	312.37	307.69	303.00	298.32	291.71	288.96
153.0	35	420.00	416.09	302.19	297.51	292.82	288.14	281.53	278.78
157.5	36	409.83	405.92	292.02	287.34	282.65	277.97	271.36	268.61
162.0	37	399.66	395.75	281.85	277.17	272.48	267.80	261.19	258.44
166.5	38	389.48	385.57	271.67	266.99	262.30	257.62	251.01	248.26
171.0	39	379.31	375.40	261.50	256.82	252.13	247.45	240.84	238.09
175.5	40	369.13	365.22	251.32	246.64	241.95	237.27	230.66	227.91

2.1.2 Clear Fiber's Length Inside the Platform.

The hole in the structure of the D0 Detector used to route cables between the detectors and the "platform" is not exactly aligned with the center of the platform. In the case of the platform housing the VLPCs there are four crates 17.5" long giving a total span of 70". If the access hole were centered it will be located in the center (between crates 2 and 3), instead it is located on top of crate 1.

This implies that a quarter of the clear fibers length must be increased by

$$\begin{aligned} 5.35 * 2.54 &= 13.589 \text{ cm} \\ 12.15 * 2.54 &= 30.861 \text{ cm} \\ 29.65 * 2.54 &= 75.311 \text{ cm} \text{ or} \\ 47.15 * 2.54 &= 119.761 \text{ cm} \end{aligned}$$

The only constraints imposed on the distribution of the fibers in the platform is that consecutive PC Boards in a crate must receive information from consecutive sectors in the CFT. A naïve routing will assign

sectors 1 through 20 to crate 2,
sectors 21 through 40 to crate 3,
sectors 41 through 60 to crate 4 and
sectors 61 through 80 to crate 1.

2.1.3 Total Clear Fiber's Lengths.

In this naïve approach to route the optical fibers their length requirements, as function of the sector of origin, is presented on Table 2.

From these values the following statistics are obtained:

Maximum total length of clear fiber	1354 cm
Minimum	709 cm
Average	976 cm

Table 2

A	B	C	D	E	F	G	H	LAYER	A	B	C	D	E	F	G	H	
									Sector #								
1265	1262	1148	1143	1138	1134	1127	1124	1	80	1354	1350	1237	1232	1227	1222	1216	1213
1255	1251	1137	1133	1128	1123	1117	1114	2	79	1344	1340	1226	1222	1217	1212	1206	1203
1245	1241	1127	1123	1118	1113	1107	1104	3	78	1334	1330	1216	1211	1207	1202	1195	1193
1235	1231	1117	1112	1108	1103	1096	1094	4	77	1324	1320	1206	1201	1197	1192	1185	1183
1225	1221	1107	1102	1098	1093	1086	1083	5	76	1314	1310	1196	1191	1186	1182	1175	1172
1215	1211	1097	1092	1087	1083	1076	1073	6	75	1303	1300	1186	1181	1176	1172	1165	1162
1204	1200	1087	1082	1077	1073	1066	1063	7	74	1293	1289	1175	1171	1166	1161	1155	1152
1194	1190	1076	1072	1067	1062	1056	1053	8	73	1283	1279	1165	1161	1156	1151	1145	1142
1184	1180	1066	1062	1057	1052	1046	1043	9	72	1273	1269	1155	1150	1146	1141	1134	1132
1174	1170	1056	1051	1047	1042	1035	1033	10	71	1263	1259	1145	1140	1136	1131	1124	1122
1164	1160	1046	1041	1036	1032	1025	1022	11	70	1253	1249	1135	1130	1125	1121	1114	1111
1153	1150	1036	1031	1026	1022	1015	1012	12	69	1242	1238	1125	1120	1115	1111	1104	1101
1143	1139	1026	1021	1016	1011	1005	1002	13	68	1232	1228	1114	1110	1105	1100	1094	1091
1133	1129	1015	1011	1006	1001	995	992	14	67	1222	1218	1104	1100	1095	1090	1084	1081
1123	1119	1005	1000	996	991	985	982	15	66	1212	1208	1094	1089	1085	1080	1073	1071
1113	1109	995	990	986	981	974	972	16	65	1202	1198	1084	1079	1075	1070	1063	1060
1103	1099	985	980	975	971	964	961	17	64	1192	1188	1074	1069	1064	1060	1053	1050
1092	1089	975	970	965	961	954	951	18	63	1181	1177	1064	1059	1054	1049	1043	1040
1082	1078	964	960	955	950	944	941	19	62	1171	1167	1053	1049	1044	1039	1033	1030
1072	1068	954	950	945	940	934	931	20	61	1161	1157	1043	1039	1034	1029	1023	1020
1106	1102	989	984	979	975	968	965	21	60	1044	1040	926	922	917	912	906	903
1096	1092	978	974	969	964	958	955	22	59	1034	1030	916	911	907	902	895	893
1086	1082	968	964	959	954	948	945	23	58	1024	1020	906	901	896	892	885	882
1076	1072	958	953	949	944	937	935	24	57	1014	1010	896	891	886	882	875	872
1066	1062	948	943	939	934	927	924	25	56	1003	999	886	881	876	871	865	862
1056	1052	938	933	928	924	917	914	26	55	993	989	875	871	866	861	855	852
1045	1041	928	923	918	913	907	904	27	54	983	979	865	860	856	851	845	842
1035	1031	917	913	908	903	897	894	28	53	973	969	855	850	846	841	834	832
1025	1021	907	902	898	893	887	884	29	52	963	959	845	840	835	831	824	821
1015	1011	897	892	888	883	876	874	30	51	952	949	835	830	825	821	814	811
1005	1001	887	882	877	873	866	863	31	50	942	938	824	820	815	810	804	801
994	991	877	872	867	863	856	853	32	49	932	928	814	810	805	800	794	791
984	980	866	862	857	852	846	843	33	48	922	918	804	799	795	790	783	781
974	970	856	852	847	842	836	833	34	47	912	908	794	789	785	780	773	771
964	960	846	841	837	832	825	823	35	46	902	898	784	779	774	770	763	760
954	950	836	831	827	822	815	813	36	45	891	888	774	769	764	760	753	750
944	940	826	821	816	812	805	802	37	44	881	877	763	759	754	749	743	740
933	930	816	811	806	802	795	792	38	43	871	867	753	749	744	739	733	730
923	919	805	801	796	791	785	782	39	42	861	857	743	738	734	729	722	720
913	909	795	791	786	781	775	772	40	41	851	847	733	728	724	719	712	709

2.2 Five - Fold Symmetry Layout.

One obvious problem with the naïve approach consist in the difficulty of managing all the clear optical fibers independently. A better approach will bundle the fibers in accordance with some ‘natural’ underling structure. One such structure is defined by the way the SF are organized in “ribbons” formed by 128 SF. For mechanical reasons it was decided (at the time of writing this D0 Note) to make the connections between the SF and the clear fibers by means of “mass terminated” connectors with densities to match the ribbon’s geometry. This creates the pattern shown on Table 3

Table 3

Layer*	Total Number of Fibers	Number of Ribbons (Connectors)	Ribbons per Geometrical Sector *
½ A	1280	10	2
½ B	1600	12.5	2.5
½ C	1920	15	3
½ D	2240	17.5	3.5
½ E	2560	20	4
½ F	2880	22.5	4.5
½ G	3200	25	5
½ H	3520	27.5	5.5
total	19200	150	30

In this approach, the clear fibers connected to the SF of each ‘GS’ form bundles that are routed to special devices called Mixing Boxes (MB), see Figure 4. The Mixing Boxes are used to rearrange the organization of the bundles so that the output of the MB is properly mapped into Trigger Sectors. The physical size of the fibers within a bundle is always the same, the length of the bundles may change.

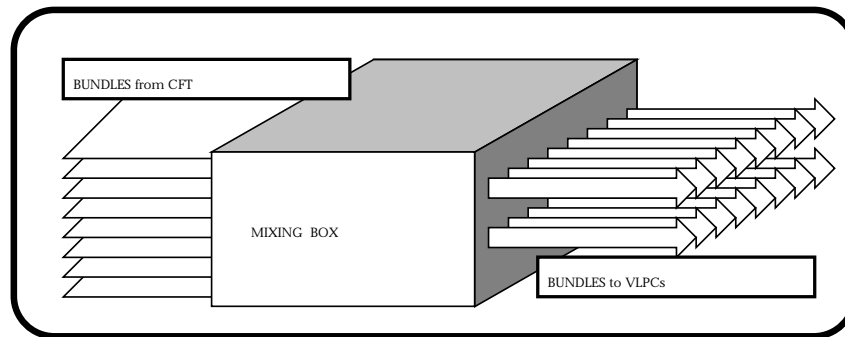


Figure 3

No information is available at this moment (July 17, 1997) regarding the size of the MBs.

* The ½ shows that the numbers correspond to the ‘inner’ or ‘outer’ portion of the layer.

* A Sector is a logical grouping of fibers created by a wedge of 4.5^0 . Each Sector is associated with a single PC Board and thus, it is the most logical division of the CFT. A “Geometrical Sector” in the contest of this paper is an ad hoc division made for mechanical simplification encompassing 16 adjacent Sectors.

For our calculations, will assume that all bundles entering and leaving the MB will do so at a single point and that the length of the box is null. Furthermore, we will assume that the MBs are located on the outer surface of the CCC and spaced 5.8^0 apart.

The position of the MBs and the Trigger Sectors serviced by them is shown on Table 4.

Table 4

Mixing Box	Φ Location	Sectors serviced	Crate Allocation
1	168.4	1 through 16	C1(1...10); C2(11...16)
2	174.2	17 through 32	C2(17...30); C4(31,32)
3	180	33 through 48	C4(33...48)
4	185.8	49 through 64	C4(49,50); C3(51...64)
5	191.6	65 through 80	C3(65...70); C1(71...80)

where $C_x (n...m)$ indicates that Trigger Sectors \underline{n} through \underline{m} are allocated to crate \underline{x} .

The apparently arbitrary allocation of Trigger Sectors to crates is explained later when the timing delays are calculated.

The information presented above is sufficient to make a good approximated calculation of the different lengths of clear fiber needed in this configuration. Clearly it is convenient to make two different calculations: one for the fibers between the SF and the MBs and another for the fibers between the MBs and the crates with the VLPCs.

2.2.1 Clear Fiber's Lengths between SF and MBs.

The distance between a SF belonging to layer $I\{A, B, C, D, E, F, G, H\}$ and Trigger Sector $s\{j...16+j\}$, and MB m is given by the expression

$$d3_1 = a_l + (R - r_l) + \pi \frac{|\phi_s - \phi_m|}{180} R + R$$

where a_l, r_l, R and Φ_s have the same meaning as before, and Φ_m is the Φ position of the MB m .

All clear optical fibers reaching the same Mixing Box \underline{m} will have the same physical length given by

$$d3_1^m = \text{Max}\{d3_1^{m,s,l}\} \quad \forall \{l\} \bullet \forall \{s \rightarrow m\}$$

The five lengths calculated using these expressions are shown on Table 5.

Table 5

Mixing Box	Clear Fiber Length Calculated	Clear Fiber Length Normalized
1	734.61	735
2	645.98	646
3	435.27	436
4	584.94	646
5	734.61	735

The third column has ‘normalized’ values to minimize the number of different lengths used.

2.2.2 Clear Fiber’s Lengths between the MBs and the VLPCs.

There is a problem here. There are five MBs and four crates; obviously it is not possible to make an one to one mapping of MBs to crates. The best that can be done is to choose between the MBs and the crates to define bundles consistent of fibers of equal length. The apparent choice is to define the bundles as function of the crates associated with them. Using this approach the length of the clear fibers (bundles) between the MBs and the crates holding the VLPCs can be written as

$$d_{m,cx} = d_{m\phi} + d_{fixed} + d_{cx} = 468.63 + d_{m\phi} + d_{cx}$$

where $d_{m\phi}$ is the length of fiber required to go from the MB m to a common point of distribution located at the outside surface of the CCC at $\Phi = 180^0$ and d_{cx} is the length of fiber needed to reach crate cx from the entrance point to the platform. Note that some decrease on the lengths needed could be obtained by ‘routing the fibers in a strait line from the MB to the vertical chimney in the holding structure of the CCC’. In this case the lengths expression became

$$d_{m,cx} = d_{m\phi} + d_{fixed} + d_{cx} = \sqrt{d_{m\phi}^2 + 55.88^2} + 412.75 + d_{cx}$$

Table 6

Trigger Sectors	MB	Crate	$d_{m\phi}$	d_{cx}	$d_{m,cx}$	Normalized
1 through 10	1	1	52.45	12.95	534.03	535
11 through 16	1	2	52.45	30.86	551.94	552
17 through 30	2	2	26.23	30.86	525.72	552
31 through 32	2	4	26.23	119.76	614.62	615
33 through 48	3	4	0	119.76	588.39	615
49 through 50	4	4	26.23	119.76	614.62	615
51 through 64	4	3	26.23	75.31	570.17	597
65 through 70	5	3	52.45	75.31	596.39	597
71 through 80	5	1	52.45	12.95	534.03	535

These values are obtained using the information provided on Table 4 and, written as function of the Trigger Sectors, are shown on Table 6.

2.2.3 Total Clear Fiber's lengths.

The total length of clear fiber that the signals must travel from the SF to the corresponding VLPC is easily obtained combining the information of tables 5 and 6 as function of sectors. This is done on Table 7

Table 7

Trigger Sectors	MB	Crate	From SF to MB	From MB to Crate	Total from SF to Crate
1 through 10	1	1	735	535	1270
11 through 16	1	2	735	552	1287
17 through 30	2	2	646	552	1198
31 through 32	2	4	646	615	1261
33 through 48	3	4	436	615	1051
49 through 50	4	4	646	615	1261
51 through 64	4	3	646	597	1243
65 through 70	5	3	735	597	1332
71 through 80	5	1	735	535	1270

For these values the following statistics are obtained

Maximum total length of clear fiber	1332 cm
Minimum	1051 cm
Average	1225.275 cm

3. Proposal for New Optical Fibers' Layout.

Three things a good routing of the optical fibers connecting the SF to VLPCs should accomplish: make all delays equal, eliminate special cases and do it at a minimal cost. In a perfect world the solution is obvious: make all optical clear fibers of equal length! Unfortunately this is impractical for two clear reasons: a) the total cost of fibers is too high, and b) there is not room to take all the extra length required by all the fibers associated with sectors other than the two located immediately before and after $\Phi = 0^0$. This idea discarded, it is necessary to find a solution where:

- the average length of the optical fibers is minimized
- the number of different lengths to be used is also minimized
- the correlation between bundles and trigger sectors is conserved as much as possible

Routing of Clear Fibers and Architecture of Front End Crates

- the difference on lengths of fibers arriving to the same crate should be minimal
- connections from crate to crate shall be such that the delay incurred by the signals going across will be less then 8 ns *
- differences on delays due to differences in clear fiber lengths shall be less then 8 ns.

It is obvious that there are contradictory conditions in this list of conditions. The solution should make a best compromise between the four conditions above mentioned. To find an appropriated routing it is convenient to start with the distribution of the sectors among the crates. The only rules to observe are:

- 1) the sectors must be organized in a linear manner within the crates, and
- 2) connections between crates must meet condition e of the previous list.

Figure 4 shows two assignments of sectors to crates. The first (Fig. 4a) one appears to be the more logic one, yet it is not a valid one because the delay introduced by the connecting cable between the first an the last crates is

$$dt_{c1,c2} = (70 + 2*(19 + 17))*2.54/29.9792458 = 12.03 \text{ ns } \heartsuit$$

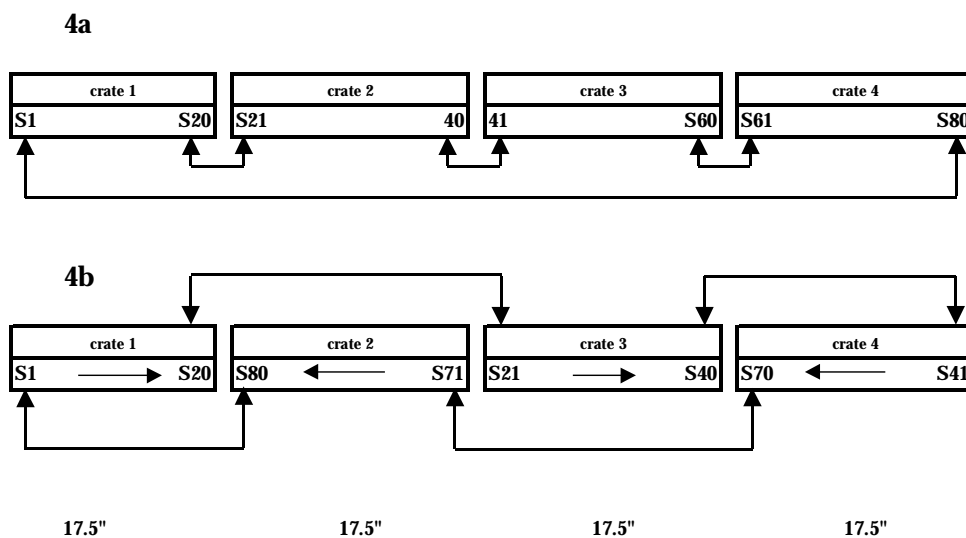
which is greater then the maximum allowed of 8 ns.

The cables needed in the second assignment (Fig. 5b) are shorter and the delays introduced by them is

$$dt_{c1,c2} = (17.5 + 2*(19 + 17 + 4))*2.54/29.9792458 = 3.25 \text{ ns } ,$$

obviously below the 8 ns allowed.

Figure 4



* This 8ns maximum allowed delay is a result of the need to have all signals arriving to the FPLDs within 8 ns of each other. This is a consequence of the four time slices used to transfer all information needed from same and adjacent sectors to the FPLDs.

♥ The numbers inside the 2*(..) correspond to the cable length needed inside the rack containing the crate.

Figure 4b also shows a possible mapping of sectors into VLPCs that tends to equalize the lengths of the clear fibers.

The next step is to try to route the clear fibers from the SF to the VLPCs without the need of MBs. As seen on the previous §, one of the problems encountered is to go from the 5-fold symmetry inherent to the MBs to a 4-fold symmetry determined by the number of crates. This problem will disappear if the number of fibers on layers B, D, F and H were multiple of 8. This is the case in the architecture proposed on D0 Note 3127. On May 1995 I proposed an architecture, named EFL3, that preserves the required multiplicity by 8 on the number of SF used on all layers (see Table 8).

Table 8

Layer	# of Fibers	Radii	Pitch in μm	Total # of Fibers	Fibers per Ribbon	# of Ribbons	Ribbons per Sector
A	16	19.0	932.66	1280	160	8	2
B	16	20.8	1021.02	1280	160	8	2
C	24	28.5	932.66	1920	160	12	3
D	24	31.2	1021.02	1920	160	12	3
E	32	38.0	932.66	2560	160	16	4
F	32	41.6	1021.02	2560	160	16	4
G	40	47.5	932.66	3200	160	20	5
H	40	52.0	1021.02	3200	160	20	5

The only difference is that now each one of the 8 layers is a “bi-layer” made of two identical “uni-layers” shifted in Φ by half the pitch. As in the rest of this paper the numbers are always referring to one ‘uni-layer’ of the layer, unless otherwise noted.

To make this architecture more in tune with the position of the layers proposed on the base-line design it is sufficient to change the radii of the layers and adjust their pitch. A possible solution is shown on Table 9 with the present solution for comparison.

Table 9

Layer	Radii		Pitch		# Fibers		# Ribbons		ometrical Sector	
	BL	EFL	BL	EFL	BL	EFL	BL	EFL	BL	EFL
A	19.50	19.50	957.2	957.2	16	16	10	8	2	2
B	23.41	23.43	919.3	1011.2	20	16	12.5	8	2.5	2
C	28.09	29.25	919.2	957.2	24	24	15	12	3	3
D	32.77	30.90	919.2	1011.2	28	24	17.5	12	3.5	3
E	37.46	39.00	919.4	957.2	32	32	20	16	4	4
F	42.14	41.19	919.4	1011.2	36	32	22.5	16	4.5	4
G	48.75	48.75	957.2	957.2	40	40	25	20	5	5
H	51.50	51.50	919.3	1150.0	44	40	27.5	20	5.5	5

Using the parameters presented on Table 9, the calculation of the clear optical fibers' lengths follows.

3.1 Clear Fibers' Lengths between the SF and VLPCs.

In a similar way as in the case of a five-fold symmetry, the clear fibers are grouped into four Geometrical Sectors defined as follows:

- sector 1 from $\Phi = \Phi_0$ to $\Phi = \Phi_0 + 90^\circ - 4.5^\circ$
- sector 2 from $\Phi = \Phi_0 + 90^\circ$ to $\Phi = \Phi_0 + 180^\circ - 4.5^\circ$
- sector 3 from $\Phi = \Phi_0 + 180^\circ$ to $\Phi = \Phi_0 + 270^\circ - 4.5^\circ$
- sector 4 from $\Phi = \Phi_0 + 270^\circ$ to $\Phi = \Phi_0 - 4.5^\circ$

where Φ_0 is chosen to minimize the overall length of the fibers and is assigned to the center of Trigger Sector 1. This makes the assignment of Sectors to crates to coincide with the one portrayed on Figure 5b. Also, each Geographical Sector is routed through a common Redistribution Area (RA) that corresponds to the MB in the five-fold symmetry. These RAs are assumed to be located on the outer surface of the CCC at the following Φ s:

- RA 1 (GS 1) $\Phi_{R1} = 185.8^\circ$
- RA 2 (GS 2) $\Phi_{R2} = 191.6^\circ$
- RA 3 (GS 3) $\Phi_{R3} = 168.4^\circ$
- RA 4 (GS 4) $\Phi_{R4} = 174.2^\circ$

Using the parameters defined above and the same expression used before

$$d3^m = \text{Max}\{d3_1^{m,s,l}\} \quad \forall \{l\} \bullet \forall \{s \rightarrow m\}$$

where now the **m** superscript corresponds to the RA, the superscripts **s, l** and the subscript have the same meaning then before. The lengths to minimize are given by

$$d_{total} = d3^m + d_{m,cx}$$

with **d_{m,cx}** defined as before.

The best results are obtained if the Trigger Sector 1 is associated with $\Phi_0 = 13^\circ 30'$. For this case

Table 10

Geometrical Sector		Trigger Sectors	Associated Crate	$d3^m$	$d_{m,cx}$	Total Length from SF to Crate	
#	Start Φ					Calculated	Normalized
1	$13^\circ 60'$	1 to 20	1	722.06	508.75	1230.81	1250
2	$103^\circ 60'$	21 to 40	3	505.24	596.71	1101.95	1105
3	$193^\circ 60'$	41 to 60	4	556.11	535.62	1091.73	1105
4	$283^\circ 60'$	61 to 80	2	772.93	472.96	1245.90	1250

For these values the following statistics are obtained

Maximum total length of clear fibers	1250 cm
Minimum	1105 cm
Average	1187.5 cm

4. Time Arrival of Signals to Trigger Boards. Delays.

One crucial parameter to take into consideration is the relative arrival times of signals to the Trigger Board. The emphasis is made on relative because the absolute timing is not an issue. Absolute delay is a parameter that affects only the starting time of the trigger calculations. Other parameter of importance is the maximum delay between the primary signal (when the signal follows a direct path) and the secondary signal (when the signal follows a path after reflection at the not connected end of the SF) independent of the layout of the optical clear fibers. Lets consider each parameter and its effect and importance.

4.1 Time Differences due to Particles' Trajectory: d1 and d2.

Referring to Figure 1 there are two path values that are independent of the layout chosen for the clear fibers: **d1** and **d2**. These delays do play an important role in the way that information can be stored, transferred and manipulated by the Trigger Board.

4.1.1 Differences due to Particle Paths (d1).

The first of variable to influence the time of arrival of signals to the Trigger Boards is due to the different trajectories of the particles from the interaction point until they strike a SF. These possible paths are function of the p-pbar interaction point $IP(0, 0, z)$ and the point $LP(0, r, c)$ where the particle interacts with the SF. Figure 6 shows three possible trajectories of a particle originating at $IP(0, 0, z)$.

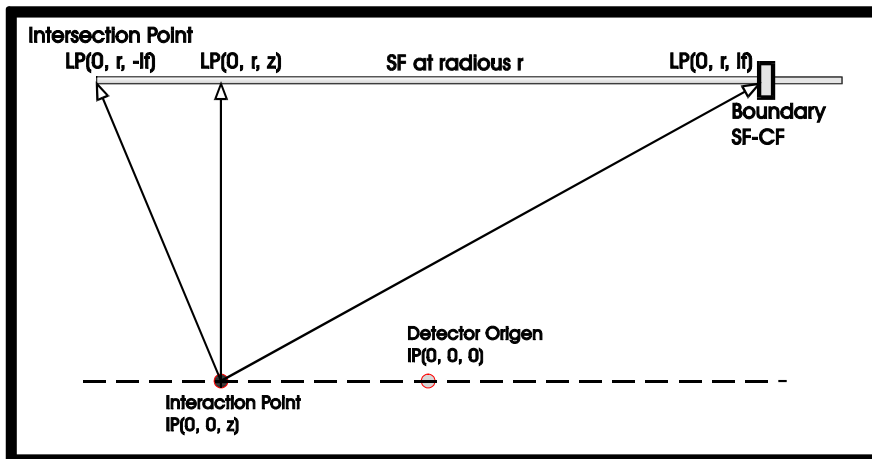


Figure 5

The length of the trajectory follow by the particle is

$$d1 = \sqrt{r^2 + (z - c)^2}$$

where r is the radius of the layer to which the SF belongs, and c is the Z -coordinate of the point where the particle strikes the SF. The following table gives values for some interesting cases

Table 11

Interaction Point			Particle Path Length in cm			Particle Path Length in ns		
			-50	0	50	-50	0	50
Layer	LP(0, R, z)							
A	19.50	-83	38.33	85.26	134.42	1.28	2.84	4.48
		-50	19.50	53.67	101.88	0.65	1.79	3.40
		0	53.67	19.50	53.67	1.79	0.65	1.79
		50	101.88	53.67	19.50	3.40	1.79	0.65
		83	134.42	85.26	38.33	4.48	2.84	1.28
H	51.5	-126	91.81	136.12	183.38	3.06	4.54	6.12
		-50	51.50	71.78	112.48	1.72	2.39	3.75
		0	71.78	51.50	71.78	2.39	1.72	2.39
		50	112.48	71.78	51.50	3.75	2.39	1.72
		126	183.38	136.12	91.81	6.12	4.54	3.06

where the path lengths are given in cm and ns. Notice that the values of z used for the interaction points (-50, 0, 50) correspond to the minimum, central and maximum values of z for accepted collisions. Interpreting the values encountered on the table we can say: particles from a single event can hit a SF from layer A as soon as .65 ns and as late as 6.12 ns after the parton interaction takes place. These values by themselves have little importance but are necessary to find the overall behavior of the Trigger Board.

4.1.2 Differences due to Effective SF Length (d2).

When a particle strikes a SF an optical signal is generated. The time which this signal takes to reach the interface between SF and clear fiber is and added delay to its time of arrival to the Trigger Board. This time is measured by $d2$ and is function of the intersection point of the particle's trajectory and the SF. The path $d2$ followed by the photons inside the SF defines an effective length of the SF. Table 12 shows these values for the same cases used in the generation of the preceding table.

Table 12

Layer	LP(0, R, z))		Photon Path length in cm		Photon Path length in ns		Difference In ns
			Direct	Reflected	Direct	Reflected	
A	19.50	-83	166	166	8.80	8.80	0.00
		-50	133	199	7.05	10.55	3.50
		0	83	249	4.40	13.21	8.80
		50	33	299	1.75	15.86	14.11
		83	0	332	0.00	17.61	17.61
H	51.5	-126	252	252	13.37	13.37	0.00
		-50	176	328	9.33	17.40	8.06
		0	126	378	6.68	20.05	13.37
		50	76	428	4.03	22.70	18.67
		126	0	504	0.00	26.73	26.73

4.1.3 Difference between Direct and Reflected Paths (Δd_2).

As mentioned in the Introduction, two different values for the path **d2** (see Fig. 1 in the Introduction) that a signal follows inside the SF must be consider: a direct path and a reflected path. The diagram shown on Figure 7 makes the point clear. A particle strikes a SF at a point P. The photons will travel along the SF following two routes. In one the photon is traveling in the direction where the connector making the interface with the clear fiber is. In this case the path length is **b**. In the other case the photon moves away from the connector, it is reflected at the end of the SF and then it moves in direction of the connector. For this case the path length is **2*a + b**. The difference between paths is then **2*a**.

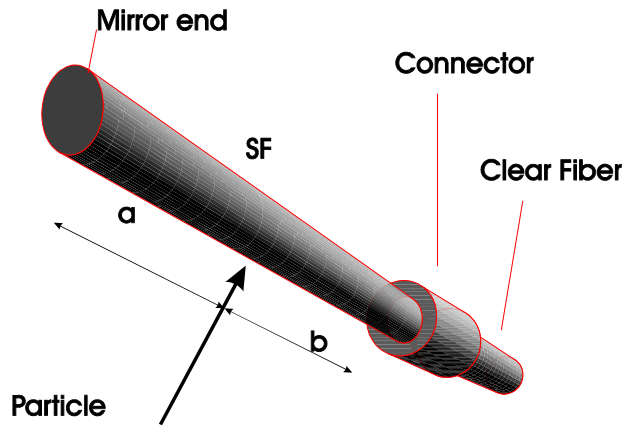


Figure 6

This is maximum when **b** is zero and **a** corresponds to the full length of the SF. The last column of Table 12 presents the difference Δd_2 of the two paths for the same cases as before.

4.1.4 Combination of both (d1 + d2).

Finally the combined delays due to the particle path and the photon path inside the SF can be obtained. Table 13 shows the results. These values, in combination with the delays encountered by the signals once they leave the SF, will be used to define the timing to store signals in the Trigger Board.

Table 13

Interaction Point			Total Signal Delay from Particle Interaction to SF CF Interface					
			-50			0		
Layer	LP(0, R, z))		Direct Path			Reflected Path		
A	19.50	-83	10.08	11.65	13.29	10.08	11.65	13.29
		-50	7.70	8.84	10.45	11.20	12.34	13.95
		0	6.19	5.05	6.19	15.00	13.86	15.00
		50	5.15	3.54	2.40	19.26	17.65	16.51
		83	4.48	2.84	1.28	22.09	20.45	18.89
H	51.5	-126	16.43	17.91	19.48	16.43	17.91	19.48
		-50	11.05	11.73	13.09	19.11	19.79	21.15
		0	9.08	8.40	9.08	22.44	21.77	22.44
		50	7.78	6.43	5.75	26.45	25.09	24.42
		126	6.12	4.54	3.06	32.85	31.27	29.79

4.2 Other Delays Independent of Clear Fibers' Routing.

Referring again to Figure 1, there are other delays that influence the time arrival of the signals to the Trigger Boards but that are independent of the path followed by the clear fibers connecting the SF to the VLPCs. From these, **d5** (delay between the input to the VLPCs and the input to the Sift Register) will affect the timings for the Sift Register. The other fixed delay (**d6**) affects only the timing of the PLDs used in the Trigger Board to 'route' the signals to the FPLDs.

As previously stated, **d5** is a simple delay generated by cables, connections and the VLPC response. Its value is approximately 2.3 ns.

The source of **d6** is a little more complex. It is a function of three different factors:

- a) delay introduced by connector(s), traces and other passive elements. Approximated value 1 ns.
- b) The time delays incurred in the Sift Chips and the connections between them and the PLDs. Approximated value 5 ns.

Unfortunately, at the time of writing this D0 Note there are not available firm values for **d5** or **d6**.

4.3 Time Differences due to Routing of Clear Fibers.

Finally, it is necessary to know the differences, as well as the absolute values, of the delays introduced by the clear fibers. It is important to catalog these in the following cases:

- 1) delay differences within the same Trigger Board
- 2) delay differences between adjacent Trigger Boards
- 3) minimum, maximum time of arrival of signals to the Trigger Boards for the total system.

These values are obtained directly from the tables already generated in the section dealing with the routing of the clear optical fibers. The tables to use are :

- Table 2 for the “naïve” routing
- Table 7 for the “5-fold symmetry” routing
- Table 10 for the “4-fold symmetry” routing

Using the data from these tables the delays and timings due to the clear fibers are obtained. They are shown on Table 14.

Table 14

Routing Type T.B. Crate	Naïve				5-fold				4-fold			
	#1	#2	#3	#4	#1	#2	#3	#4	#1	#2	#3	#4
Max. Δdelay withing a Trigger Board	7.48				0				0			
Max. Δdelay between Trigger Boards within the same Crate	8.01				0	4.72	4.72	11.14	0			
Min. Delay among all signals	37.67				55.74				58.61			
Max. Delay among all signals	71.83				70.64				66.30			
Max. Δdelay among all signals	34.16				14.90				7.69			

4.4 Total Delays and Time Differences.

Without taking into account the differences of arrival between the direct signals and the reflected ones, the following chart of delays and time differences emerges. It suffices to combine the information presented on Table 14 with the values shown on Table 13. This is shown on Table 15. The way these values are obtained is by:

Adding 18.2 ns to the first two rows of Table 14. This value is the difference between the maximum and minimum delays from signals following a direct path as shown on Table 13

Adding to the third row of Table 14 the minimum delay of 1.28 ns from the direct path columns on Table 13.

Adding to the four row of Table 14 the maximum delay of 19.28 ns from the direct path columns on Table 13.

Note that only the direct signals delays and timings are needed.

Table 15

Routing Type T.B. Crate	Naïve				5-fold				4-fold			
	#1	#2	#3	#4	#1	#2	#3	#4	#1	#2	#3	#4
Max. Δ delay withing a Trigger Board	25.68				18.2				18.2			
Max. Δ delay between adjacent Trigger Boards within same Crate	26.21				18.2	22.92	22.92	29.34	18.2			
Min. Delay among all signals	38.95					57.02			59.89			
Max. Delay among all signals	90.91					89.72			85.38			
Max. Δ delay among all signals	51.96					32.70			25.49			

5. Making Sense of the Numbers.

All the values obtained in the previous sections tell us several stories. One story for each type of filter used in their interpretation. Two main questions are of importance here:

- a) how these values affect the timing and implementation of the Trigger Board
- b) how they relate to the total cost of the system.

5.1 Trigger Board Timing Requirements.

There are several timing signals of great importance in the design and proper functionality of the Trigger Board. The Trigger Board must decide when start acquiring data from the SF and for how long, when to transfer data from the Sift Chip to the routing PLDs and to the SVX chips, when to transfer data from the PLDs to the FPLDs, when to send information to the μ -trigger and to the Level 1 Trigger, etc.

To understand how the signal timing and delays affect the design of the Trigger Board it is necessary to have a good understanding of its functions. More specifically, we must know how the signals generated by the SF are treated in the Trigger Board.

The descriptions that follow are based on a 132 ns crossing time.

5.1.1 Data Acquisition by the Trigger Board.

The optical signals generated in the SF arrive to the Trigger Board after conversion to electrical pulses by the VLPCs. For each SF belonging to a Trigger Sector there is an input data channel dedicated to it in the Trigger Board. The best way to obtain a good understanding of the requirements imposed on the Trigger Board is to follow a signal through it. The analog data is routed to an specially designed chip: the Sift Chip. For each input signal the Sift Chip outputs two: an analog amplified copy of the input and a digital signal. Figure 8 is a very simplified functional block diagram of the Sift Chip and the hardware/functions associated with it. Figure 9 is a very simplified timing diagram for the Sift Chip. Of the five control clocks needed by the chip only the three necessary to understand the constrains imposed on the system are shown.

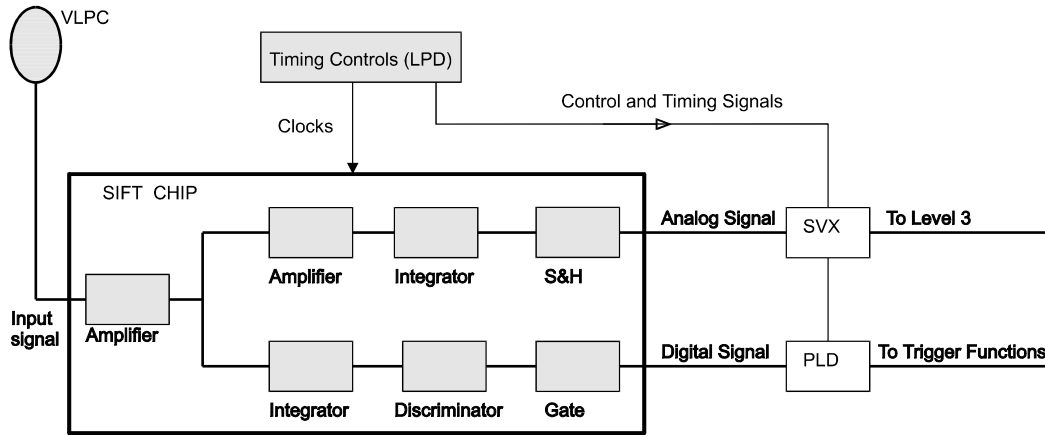


Figure 7

First a brief description of the Sift Chip behavior. The cycle starts at some point in time, let's say $t = t_0$. The events that take place are as follows:

t_0) the Sift Chip is reset. PRST and DRST change from 0 to 1

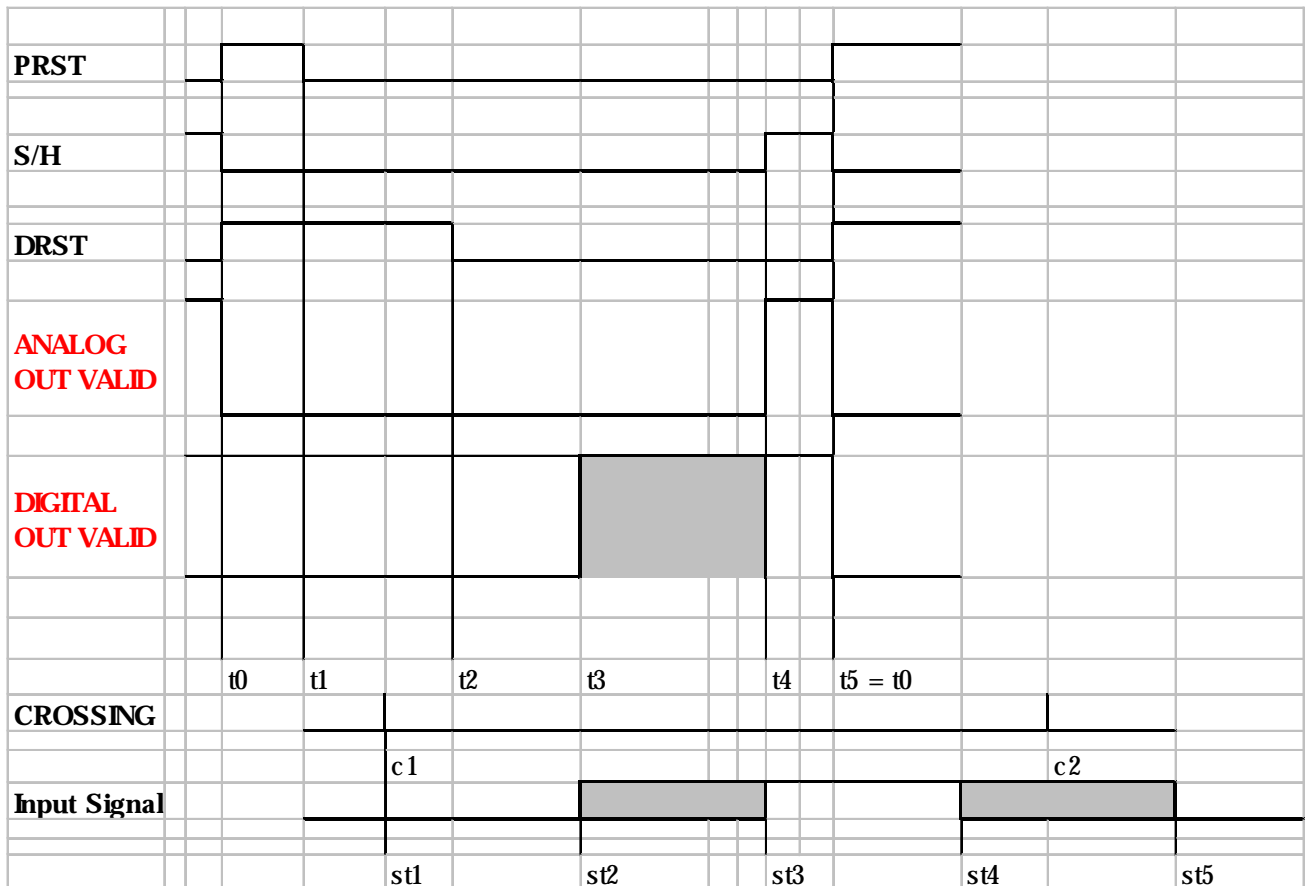


Figure 8

t_1) after 25 ns PRST change from 1 to 0. The input signal is integrated along the 'analog' path. 25 ns elapsed from t_0 .

Routing of Clear Fibers and Architecture of Front End Crates

t_2) 45 ns after t_1 DRST returns to 0, integration of the input signal along the ‘digital’ path starts. Integration along the ‘analog’ path continues. 70 ns elapsed since t_0 .

t_3) some time after t_2 the integrator value could reach a preset threshold value. When this occur the digital output became a 1. The discriminator will remains 0 as long as the integrated function is below a preset threshold value.

t_4) no later then 117 ns after t_0 the sample and hold is activated and integration functions stop. Both analog and digital outputs are stable. They reflect the status of the ‘analog’ integration and the discriminator at the moment of activation.

t_5) cycle restart. $t_0 < t_4$. Time elapsed 132ns.

During this cycle the crossing cycle is taking place. The Trigger Board receives two clock signals from the Trigger Framework for synchronization:

- 1) the 53MHz system clock
- 2) a signal concurrent with the crossing signal

5.1.2 When to Start the Trigger Time.

For the system to provide valid information the timing of the Sift Chip needs to meet two conditions:

- 1) The time interval between t_1 and t_4 must be sufficient to allow for 95% of the signal to be integrated. This ensures that the data presented to the SVX is a good representation of the output of the VLPC.
- 2) The time interval between t_2 and t_4 must be sufficient to allow for the discriminator to do its job.

It is clear that *all* functions that the Trigger Board performs *must be perfectly synchronized* with the time of *data arrival*. In particular, timing cycles of the Sift Chip must start well after the time c_n when the collision takes place. This is so because data arrives to the Sift Chip some time after the collision takes place and, thus, some time after c_n . The beginning of the Sift Chip cycle can not start at the same time that the crossing time. Specifically, the position of t_1 from the Sift Chip cycle must be as close as possible to the arrival of data.

By measurements done using SF 2.5 m long connected by a clear fiber to a VLPC the rise time and decay have been found to be ~ 60 ns. To assure that the Sift Chip integrator “sees” ~95% of the signal the acquisition time required by the Sift Chip is

$$\begin{aligned} t_{acquisition} &= \max\left\{t_{arrival}^{reflected} - t_{arrival}^{direct}\right\} + t_{integration}^{95\% \text{ area}} = \\ &= 26.73 + 60 = 86.73 \text{ ns} \end{aligned}$$

The time delays of conduits and Sift Chip combined are of the order of 3 to 5 ns. Adding all these three delays a value for d_6 is obtained:

$$d_6 = 2.3 + 86.73 + 5 \sim 94 \text{ ns.}$$

The optimal value for the integration time was already calculated on §2.2 . There the acquisition time was given as

$$\begin{aligned} t_{\text{acquisition}} &= \max \left\{ t_{\text{arrival}}^{\text{reflected}} - t_{\text{arrival}}^{\text{direct}} \right\} + t_{\text{integration}}^{95\% \text{ area}} = \\ &= 26.73 + 60 = 86.73 \text{ ns} \end{aligned}$$

Due to timing problems encountered with the actual Sift Chip this value has been fixed to some shorter time. The acquisition time used by the Trigger Board is:

$$t_{\text{acquisition}} = 70 \text{ ns}$$

This implies a degradation in the accuracy of triggers using the SF data. This is because the % of the area of the reflected signal integrated by the Sift Chip depends of the difference of arrival times of the direct and the reflected signals. It is totally possible to *miss* some events by the Level 1 Trigger due to this. Also the accuracy of the measurement of the *strength* of the signal is affected. On the other hand, the true strength of the signal can be calculated at the Level 3 by knowing where the particle struck the SF and, thus, calculating the time differential between direct and reflected signals.

6. Comparison of Routing Schemes.

6.1 Comparison with the Naïve Layout.

Using the five-fold symmetry several improvements are achieved over the naïve arrange, among them:

- 1) The number of different lengths for the clear fibers is drastically reduced from about 9600 to seven; three different lengths from the SF to the MBs and four different lengths going from the MBs to the crates
- 2) The fact that bundles of fibers are identified with the MBs or the crates makes the bookkeeping a lot simpler.

On the other hand, the usage of the MBs introduces a new complications and expenses. Some of these are listed below:

- 1) It is necessary to design and build another piece or hardware; the MB. It design and implementation is far from simple.
- 2) The usage of the MB introduces additional cost because four more mass terminated optical connectors are needed.
- 3) The usage of the MB introduces additional complexity and unreliability in the system because two more optical interfaces are needed.

Routing of Clear Fibers and Architecture of Front End Crates

- 4) There is an additional cost incurred in clear fibers. The average length of a clear fiber with the naïve approach was 976 cm and with the five-fold symmetry is of 1225.275 cm; this increase the clear fiber cost by

$$249.275 * 19200 * 2 * (\text{optical fiber cost per cm})$$

These factors are sufficient to investigate the possibility of a different organization where the usage of MBs is not needed.

6.2 Comparison between 5-fold and 4-fold geometry.

It is very helpful to make a comparison between the two viable geometries in order to make a knowledgeable choice between them. The best way to compare them is to provide a list of the features of both. This is done on Table 11.

Table 16

Parameter Layer	Radii		# of fibers		Pitch in μ		# of Ribbons	
	5-fold	4-fold	5-fold	4-fold	5-fold	4-fold	5-fold	4-fold
A	19.50	19.50	2*16	2*16	957.2	957.2	10.0	8
B	23.41	23.43	2*20	2*16	919.3	1011.2	12.5	8
C	28.09	39.25	2*24	2*24	919.2	957.2	15.0	12
D	32.77	30.90	2*28	2*24	919.2	1011.2	17.5	12
E	37.46	39.00	2*32	2*32	919.4	957.2	20.0	16
F	42.14	41.19	2*36	2*32	919.4	1011.2	22.5	16
G	48.75	48.75	2*40	2*40	957.2	957.2	25.0	20
H	51.50	51.50	2*44	2*40	919.3	1150.0	27.5	20

The total number of SF needed is decreased from 38400 to 35840. The usage of less number of SF and of a 4-fold symmetry results in:

- 1) savings in SF, clear fibers, connectors, etc.
- 2) no need for usage of half ribbons to cover the detector
- 3) no need of using half mass terminated connectors
- 4) no need to use Mixing Boxes **

** The need for Mixing Boxes in the case of a 5-fold symmetry can be eliminated by the design of a suitable geometry and an "Electronic Mixing Matrix". The complication arises from the need to split bundles for the B, D, F and H sectors.